nell University Press: Ithaca, NY, 1979.
(43) Quigg, C.; Rosner, J. L. *Phys. Rep.* **1979**, *56*, 167. The virial theorem for power law potentials is nicely treated in this work while the δ-function surface interaction pseudopotential is also shown to satisfy the virial relation in ref 14a. A proof for the whole class of homogeneous one-body potentials has not been given, but results obtained so far are consistent with the relation given in the text. For an application of the virial theorem to a many-body Hamiltonian along with caveats, see: Hefter, E. F.; Mitropolsky, I. A. *Nuovo Cimento* **1986**, *95A*, 63.
(44) (a) Anderson, P. W. *Proc. Natl. Acad. Sci. U.S.A.* **1972**, *69*, 1097. (b) Mott, N. *J. Phys. C* **1987**, *20*, 3075. (c) McKane, A. J.; Stone, M. *Ann. Phys.* **1981**, *131*, 36. (d) Abrams, E.; Anderson, P. W.; Licciardello, D. C.; Ramakrishnan, T. W. *Phys. Rev. Lett.* **1979**, *42*, 693.
(45) Cohen, M. H.; Economou, E. N.; Soukoulis, C. M. *Phys. Rev. B* **1985**, *32*, 8268.
(46) Donsker, M. D.; Varadhan, S. R. S. *Commun. Pure Appl. Math.* **1975**, *28*, 1; 279; 525; **1979**, *32*, 721.
(47) Ezawa, H.; Klauder, J. R. *J. Math. Phys.* **1975**, *16*, 783.

Effect of Polymer Chain Microstructure on Solvent Crystallization: Implications on Polymer Solvation and on Physical Gelation

Marc Klein and Jean-Michel Guenet*,†

Institut Charles Sadron, CNRS—Université Louis Pasteur, 6, rue Boussingault, 67083 Strasbourg Cedex, France. *Received July 18, 1988; Revised Manuscript Received February 16, 1989*

ABSTRACT: In this paper we determine by means of the solvent crystallization method the degree of polymer solvation through the parameter $\bar{\alpha}$, which is the average number of solvent molecules per monomer. For polymers possessing side groups such as poly(methyl methacrylate), poly(hexyl methacrylate), and polystyrene there is a simple relation between $\bar{\alpha}$ and the solvent size. For polymers without side groups such as poly(dimethylsiloxane) or poly(vinyl chloride) there is no relation. These results are interpreted with the notion of a cavity formed by the side groups. Temperature–concentration phase diagrams are established for the different polymers in *p*-chlorotoluene. Departures from theoretical solvent melting point depression (Flory) are also accounted for by the notion of cavity. The cavity's effect is examined as to its relevance for understanding the physical gelation of polymers possessing side groups.

Introduction

The interactions between a polymer and a solvent have been and still are widely studied. They constitute an important chapter in the study of amorphous polymer solutions.[1-4]

These interactions also play an important role when crystallizable polymers are dealt with. For instance poly(ethylene oxide) (PEO) can crystallize from solutions either under an "anhydrous" form or under a "solvated" form.[5,6] In the case of PEO–para-disubstituted benzene mixtures, Point et al.[7] have shown that a polymer–solvent compound is produced rather than the "anhydrous" form. According to Point et al.[7] this is so because the solvent molecule adapts perfectly within the shape of the helical form adopted by the polymer. As a result, the compound melts at a temperature higher than that of either component. Similar conclusions have been drawn for syndiotactic poly(methyl methacrylate) (sPMMA).[8]

The same mechanism is thought to occur in physical gelation of stereoregular polymers.[9-11] In this respect, the case of isotactic polystyrene/*cis*-decalin gels is worth mentioning since it has been deeply investigated by different techniques. The temperature–concentration phase diagrams[12] show that gelation arises from the formation of a congruently melting polymer–solvent compound. From neutron diffraction experiments,[11] it is concluded that the compound owes its formation to the cavities formed by the benzene rings: solvent molecules that can enter these cavities can form physical bridges between different chains. The same conclusion is drawn from the study of the solvent crystallization behavior once the gel is produced.[11] A relation has been established between the degree of solvation and the molecular size.

The purpose of this paper is manifold and aims particularly at (i) testing more deeply the reliability of the solvent crystallization method,[11,13] (ii) cross-examining the notion of cavity with other polymers possessing or not possessing bulky side groups, (iii) investigating the problem on a theoretical basis, and (iv) assessing the role of the cavity in the phenomenon of thermoreversible gelation.

As with isotactic polystyrene,[11] we shall examine these points by studying the solvent melting behavior in various types of polymer–solvent mixtures including stereoregular and stereoirregular polymers.

Theoretical Section

1. Polymer–Solvent Phase Diagrams. Whether a polymer is crystallizable or not, different phase diagrams can be obtained as described, in detail, by Pakpov.[14]

(a) If the polymer is liable to crystallize, two schematic types of phase diagrams can be obtained: (i) the polymer crystallizes under an "anhydrous" form which entails rejection of the solvent into the amorphous part leading to the formation of a solid solution (Figure 1a); (ii) the polymer and the solvent cocrystallize so as to form a polymer–solvent compound that melts either congruently or incongruently (Figure 1b).

In both cases, C_E represents the concentration at which an eutectic mixture is formed between the solvent and the crystallized polymer (Figure 1a) or the solvent and the polymer–solvent compound (Figure 1b). In this paper we consider situations where the discrepancy between the melting point of either the polymer or the polymer–solvent compound, on the one hand, and the solvent, on the other hand, is large (over 100 °C). Consequently, and as was experimentally shown for oligomers,[15,16] the eutectic concentration C_E is shifted toward zero, which entails a merge

†Present address: Laboratoire de Spectrométrie et d'imagerie ultrasonore, Université Louis Pasteur-CNRS, 4, rue Blaise Pascal, F-67070 Strasbourg Cedex, France.

0024-9297/89/2222-3716$01.50/0

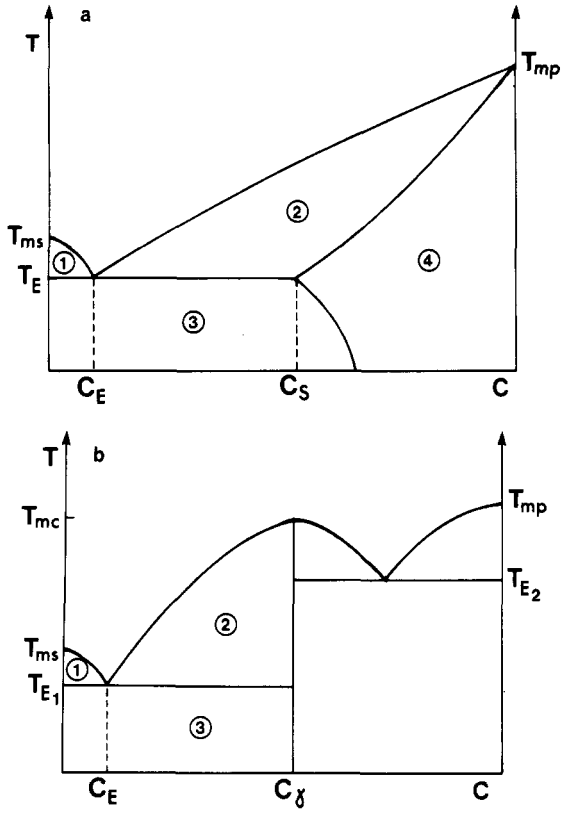

Figure 1. (a) Theoretical temperature–concentration phase diagram with formation of a solid solution (domain 4), domain 1 = solvent crystals + liquid, domain 2 = liquid + solid solution, and domain 3 = solvent crystals + solid solution. (b) Theoretical temperature–concentration phase diagram with formation of a congruently melting compound. Domain 1 = solvent crystals + liquid, domain 2 = liquid + compound, and domain 3 = solvent crystals + compound.

of the solvent melting line and the eutectic line ($T_{m_s} \simeq T_E$). As a result, it is experimentally found that the solvent melting point is invariant with concentration although, strictly speaking, one is determining the eutectic line.[11,12]

(b) If the polymer does not spontaneously crystallize, then the phase diagrams will resemble that of Figure 2. Note that in this case there will be interferences with the T_g line if any.

The goal of this paper is concerned with the study of the solvent melting behavior. In the case of Figure 1, the line at T_{m_s}, as explained above, is a constant. Conversely, in the case drawn in Figure 2 this line decreases with increasing concentration. In principle, this solvent melting line can be calculated from the Flory–Huggins[1] relations from the solvent chemical potential per mole $\Delta\mu_s$, as a function of the solvent volume fraction v_s and the interaction parameter χ:

$$\Delta\mu_s = RT_{m_s}[\log v_s + (1 - v_s) + \chi(1 - v_s)^2] \quad (1)$$

At the melting temperature T_m, provided there is no change of heat capacity from the solid to the liquid, we also have

$$\frac{\Delta\mu_s}{T_{m_s}} = \Delta H_{0s}\left[\frac{1}{T_{m_s}^\circ} - \frac{1}{T_m}\right] \quad (2)$$

in which T_{m_s} and $T_{m_s}^\circ$ are the melting temperatures of the solvent in the polymer–solvent mixture and the pure solvent, respectively, and ΔH_{0s} is the heat of fusion of the pure solvent. Equating (1) and (2) finally yields[17]

$$\frac{1}{T_{m_s}} - \frac{1}{T_{m_s}^\circ} = -\frac{R}{\Delta H_{0s}}[\log v_s + (1 - v_s) + \chi(1 - v_s)^2] \quad (3)$$

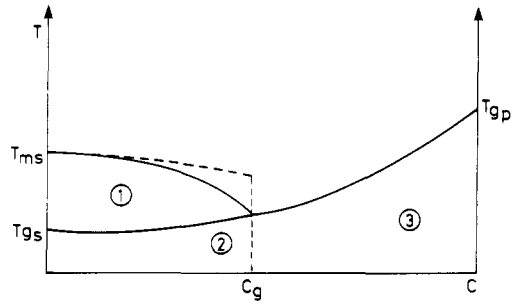

Figure 2. Theoretical temperature–concentration phase diagram for an amorphous polymer in solution. Domain 1 = solvent crystals + polymer solution, domain 2 = solvent crystals or glassy solvent + glassy polymer solution, and domain 3 = glassy polymer solution. Dotted line represents the case with a discontinuity at C_g.

The χ parameter is known to be dependent upon concentration, temperature, and molecular weight. Koningsveld and Kleintjens[18] have proposed to express the concentration dependence of χ by

$$\chi = \delta + \frac{\beta(1 - \gamma)}{(1 - \gamma v_s)^2} \quad (4)$$

where δ and γ are constants and β varies linearly with $1/T$. From the solvent vapor pressure of polymer solutions, it has been found that the variation is between 0.3 and 0.8, depending upon solvent and concentration.[19-22]

As to the glass transition line, its variation $T_g(v_s)$ with the solvent volume fraction v_s can be calculated from the relation determined by Kovacs and Braun:[23]

$$T_g(v_s) = \frac{v_s\Delta\alpha_s T_{g_s} + (1 - v_s)\Delta\alpha_p T_{g_p} + kv_s(1 - v_s)}{v_s\Delta\alpha_s + (1 - v_s)\Delta\alpha_p} \quad (5)$$

in which $\Delta\alpha_s$ and $\Delta\alpha_p$ are the variation from the glass to the liquid of the dilatation coefficients of the solvent and the polymer, respectively, T_{g_s} and T_{g_p} are the glass transition temperatures of the solvent and the polymer, respectively, and k is a constant related to the polymer–solvent interactions (according to Kovacs and Braun,[23] k lies within $0 < k < 0.015$).

By means of relations 3 and 5, it is in principle possible to calculate the type of phase diagram drawn in Figure 2 from the knowledge of a minimum number or parameters, among which are the polymer–solvent interaction parameters.

2. Polymer Solvation. For all the situations represented in Figures 1 and 2, there is a concentration beyond which "free" solvent molecules no longer remain.[11,13] Then the notion of polymer solvation can be put forward. This notion does not imply that the solvent molecules are trapped along the chain and motionless but simply that they undergo a polymer–solvent interaction preventing them from forming solvent crystals. Sometimes these solvent molecules are said to be "bound" to the polymer.

The concentration at which this occurs can be experimentally determined by studying the solvent melting enthalpy ΔH_s. ΔH_s can be expressed as a function of the pure solvent melting enthalpy ΔH_{0s} and the polymer concentration C (in g/g):[11]

$$\Delta H_s = \Delta H_{0s}\{1 - C[1 + \bar{\alpha}ms/mp]\} \quad (6)$$

where ms and mp are the molecular weight of the solvent and the monomer unit, respectively, and $\bar{\alpha}$ is a parameter that is the average number of solvent molecules per mo-

Table I

solvent	V_m, cm^3	ΔH_{0s}, cal/g	mp, °C	no. in Figure 4
acetonitrile	52	43.34	−48	16
carbon disulfide	60	13.95	−111.5	9
methylene chloride	63	17.87	−97	2
1,2-dichloroethane	79	22.10	−35	1
chloroform	80	18.36	−60	7
benzene	89	28.76	+5.5	4
chlorobenzene	101	22.11	−45	5
bromobenzene	105	16.10	−31	17
toluene	106	17.20	−95	21
cyclohexane	108	7.48	+6.55	22
o-dichlorobenzene	112	20.73	−15	6
p-chlorotoluene	118	23.89	+6	10
cyclohexane	118	9.74	−104	8
o-xylene	120	27.01	−25	20
p-xylene	123	35.03	+12	3
2-chloro-*p*-xylene	132	27.36	+4	11
diethyl oxalate	136	24.99	−41	19
bromonaphthalene	140	13.60	−1	18
cis-decalin	154	14.65	−43	12
trans-decalin	159	22.71	−30	13
chlorodecane	200	32.82	−34	14
chlorododecane	237	36.00	−9.3	15

nomer unit. Concerning cases of Figures 1b and 2, $\bar{\alpha}$ is given by

$$\bar{\alpha} = \frac{1 - C_0}{C_0} \frac{\text{mp}}{\text{ms}} \tag{7}$$

where C_0 is the polymer concentration for which $\Delta H_s = 0$.

Concerning the case of Figure 1a, the fact that the crystalline domains do not contain solvent molecules any longer leads to correction of relation 7 for calculating the true polymer solvation in the amorphous domains. Accordingly, $\bar{\alpha}$ reads

$$\bar{\alpha} = \frac{1 - (1 - x)C_0}{(1 - x)C_0} \frac{\text{mp}}{\text{ms}} \tag{8}$$

where x is the degree of crystallinity.

Note that the concentration C_0 at which all the solvent molecules are "bound" corresponds to C_s for the case of a solid solution, to C_γ in the case of a polymer–solvent compound, and to C_g in the case of an amorphous polymer. For the latter, we admit that the solvent melting line and the T_g line intersect at the concentration C_g at which all the solvent is "bound". This point is conjectural at the moment. It mainly relies upon the idea that as long as there are free solvent molecules that can crystallize, the system cannot lie under its T_g. In other words, since there are two phases (the solvated polymers plus free solvent), for the whole system to be under its T_g requires that both phases be under their glass transition temperature. With most solvents, it is virtually impossible under the experimental conditions described above to reach their T_g before crystallization, and then the above requirement cannot be fullfilled. Conversely, at C_g and beyond only one phase remains (solvated polymer) which is more liable to undergo a vitreous transition. It must be stressed that another situation can be envisaged: all the solvent can be "bound" yet the system can always lie well-above its glass transitions. Then we should observe a discontinuity at T_g between the solvent liquidus line and the T_g line (see Figure 2, dotted line).

Experimental Section

1. Materials. The solvents were selected in order to have access to a wide range of solvent molar volumes (see Table I). All the solvents, from different origins, were of high purity grade and were used without further purifications.

Table II

polymer	M_w, g/mol	M_w/M_n	tacticity, % i	s	h	origin
aPS	2.90×10^5	<1.2	20	63	17	this lab
iPMMA	3.65×10^4	3.79	89	5	6	Röhm GmBH
sPMMA	1.06×10^5	2.86	10	66	24	
PHMA	6.02×10^4	1.13				this lab
PVC	1.20×10^5	2.30	18	33	49	Rhône-Poulenc S.A
PDMS	2.50×10^4					

The following polymers, whose characteristics are gathered in Table II, were used: atactic polystyrene (aPS), isotactic polystyrene (iPS), isotactic poly(methyl methacrylate) (iPMMA), syndiotactic poly(methyl methacrylate) (sPMMA), atactic poly(hexyl methacrylate) (PHMA), poly(dimethylsiloxane) (PDMS), and atactic poly(vinyl chloride) (PVC).

2. Techniques. The determination of both the heat of fusion and the melting point of the solvent were carried out on a Perkin-Elmer DSC2 calorimeter equipped with the thermal analysis system TADS. Calibrations of energy and of temperature scale were achieved by means of indium and gallium standard samples. Heating and cooling rates ranged from 2.5 to 20 °C/min. The phase diagrams were established by extrapolating to zero heating rate.

Optical micrographs were taken with a Zeiss photomicroscope. The samples were cooled to low temperature by means of a Mettler hot stage operating with a flux of cool, gaseous nitrogen. The temperature as well as the heating and cooling rates (typically 1 °C/min) was monitored by the Mettler FP80 central processor.

3. Sample Preparation. For amorphous polymers such as aPS, iPMMA, sPMMA, PHMA, and PDMS, the polymer–solvent mixtures were prepared directly into "volatile sample" pans. A desired quantity of polymer was introduced into a weighed pan; then an estimated volume of solvent was added. Once tightly sealed, the pans were weighted so as to calculate the concentration and also to test whether any loss of solvent occurred during the aging period. Aging took place at room temperature for approximately 2 months so as to obtain homogenous samples. Some DSC measurements were repeated 1 month later in order to verify that homogeneous samples were dealt with.

Concerning iPS and PVC, which tend to give physical gels, the samples were first prepared in a test tube then introduced into a volatile sample pan. As a result, no aging was needed to ensure homogeneity.

4. Solvent Crystallization Procedure. Since the entire analysis relies upon the correct determination of ΔH_s, it is of importance that the free solvent molecules be all crystallized. Due to the use of polymers, high viscosity solutions are dealt with, which may result in partially hampering or in slackening up crystallization of the free solvent molecules. Accordingly, various crystallization procedures must be brought about in order to make sure that crystallization of all the free solvent molecules did take place.

We used the following procedures: crystallization at different and very slow cooling rates (−5, −2.5 °C/min) and comparison of the solvent heat of fusion obtained on heating for either crystallization condition; crystallization at 20 °C/min, then annealing close to the solvent melting point for 10, 20, and 30 min, cooling down again, and heating at 20 °C/min.

Generally, effects less than 10% were observed on the value of ΔH_s. Only the case of 1,2-dichlorobenzene showed significant variation, especially after annealing.

Worth emphasizing is that a linear variation of ΔH_s as a function of C (relation 6) is a good criterion to assess the correctness of the measure of $\bar{\alpha}$. Should there be any experimental problems such as incomplete crystallization of the free solvent, this would give rise to significant departure from linearity. This was experimentally observed for atactic polystyrene in mesitylene. As a result this solvent was disregarded.

5. Accuracy of the Determination of $\bar{\alpha}$. The experimental error in $\bar{\alpha}$, $\Delta\bar{\alpha}$, is expressed as

$$\Delta\bar{\alpha} = \bar{\alpha}\frac{\Delta C_0}{(1 - C_0)C_0} \tag{9}$$

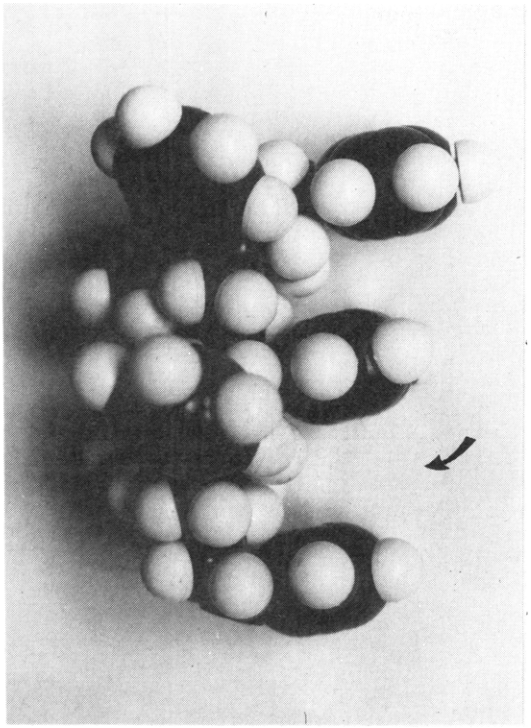

Figure 3. Representation by means of molecular models of a isotactic polystyrene chain under a near-3_1 helical form. Arrow indicates the cavity.

As can be seen, the error is minimum around $C_0 \simeq 0.5$. Departure from this value entails larger and larger errors. For instance, if we take $\Delta C_0 \simeq \pm 0.03$, which is the usual uncertainty due to experimental scatter, we see that if $\bar{\alpha} \simeq 3$ with $C_0 = 0.3$, then $\Delta\bar{\alpha} \simeq \pm 0.42$. If $\bar{\alpha} \simeq 0.3$ with $C_0 \simeq 0.8$, then $\Delta\bar{\alpha} \simeq \pm 0.06$. These estimates show that the relative error $\Delta\bar{\alpha}/\bar{\alpha}$ reaches values of 14% to 20% in extreme cases.

Results and Discussion

1. Solvent Characteristics. It has been shown in iPS physical gels[11] that there is a simple relation between the value of $\bar{\alpha}$ and the solvent molar volume V_m. From this result the notion of a cavity, formed by the phenyl groups along the chain, was put forward (Figure 3). If the solvent is larger than the cavity it cannot enter the latter without deforming it. The deformation of one cavity can reduce the available volume of the adjacent one. Accordingly, this adjacent cavity is no longer accessible to the solvent. In the end, this effect should lead to a lower average degree of solvation since some cavities will not contain solvent molecules any longer. Conversely, if the solvent is smaller it can fit in this cavity, hence a higher value of $\bar{\alpha}$.

We have used, as far as possible, solvents possessing melting points in a narrow range of temperature, usually around room temperature. Yet, for the solvents of smallest molar volume the melting point inevitably lies at a lower temperature. However, in all cases the interaction parameter does not vary drastically with decreasing temperature. Also, the use of *p*-xylene or *o*-xylene with aPS did not point out any significant difference, although the melting points of these solvents are some 37 °C apart.

In Figure 4 are drawn the exotherm of the solvent crystallization and the melting endotherm for a high concentrated solution. This illustrates, unlike what is commonly thought, that the solvent crystallization is not necessarily strongly hampered under these conditions.

We have also noticed that the solvent crystallization method allows comparison between $\bar{\alpha}$ and V_m if another condition is fulfilled. As can be seen in Figure 4, for a majority of solvents a simple linear relation is found between the molar volume and the molar enthalpy. This expresses that the density of melting enthalpy is a constant. Yet, some solvents do not obey this rule. For instance, *cis*-decalin, cyclohexane, and cyclohexene are well above this line while acetonitrile is well below. We have experimentally noticed that these solvents do not comply to the relation between the solvent molar volume V_m and $\bar{\alpha}$. *cis*-Decalin, cyclohexane, and cyclohexene tend to give values of $\bar{\alpha}$ that are larger than expected and the reverse situation is seen for acetonitrile.

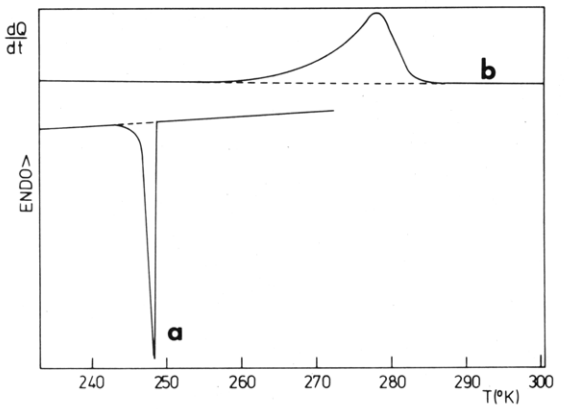

Figure 4. DSC thermogram of a 49.86% mixture iPMMA–*p*-chlorotoluene. Lower curve (a) shows the crystallization exotherm of the solvent (cooling rate 5 °C/min) and upper curve (b) the melting endotherm of the solvent (heating rate 10 °C/min).

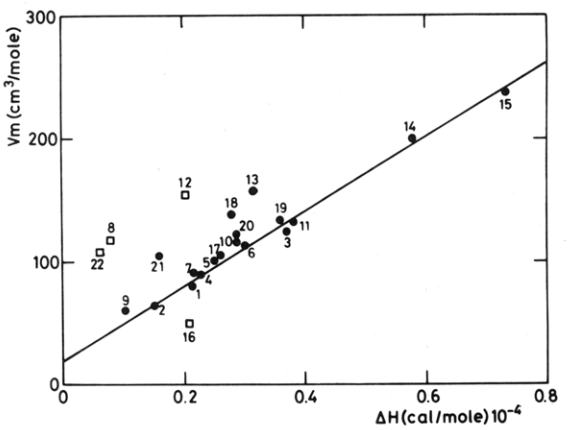

Figure 5. Representation of the solvent molar volume as a function of solvent molar enthalpy. Numbers correspond to solvents listed in Table II. Squares are for solvents that show the highest discrepancy from the linerar variation.

The following interpretation may account for these results: for solvents located above the line $V_m = \Delta H_s C^{ste}$ (Figure 5), the crystal cohesive energy is weaker than normal, which indicates that the polymer–solvent interaction may be large enough to prevent crystallization, hence a larger value of $\bar{\alpha}$. Conversely, for solvents located below this line, the crystal cohesive energy is higher than normal, which may lead to partial polymer desolvation with solvent crystallization, hence a lower value of $\bar{\alpha}$.

Finally, the solvent molar volume to be considered ought to be that determined at the melting point. Here we have used the values at 20 °C that are available from any chemical handbook. The maximum discrepancy between the values at 20 °C and at the melting point is about 20% for solvents of very low melting points such as CS_2 or CH_2Cl_2 and 10% for the other solvents. We therefore decided not to correct the results to a first approximation.

2. Relation between $\bar{\alpha}$ and V_m. Typical results of the melting enthalpy vs polymer concentration are drawn in Figure 6 for PMMAs in *p*-chlorotoluene. As can been seen,

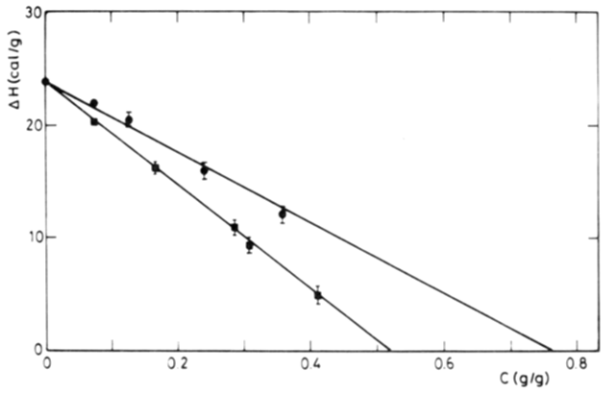

Figure 6. Solvent melting enthalpy (*p*-chlorotoluene) vs polymer concentration: (■) sPMMA and (●) iPMMA.

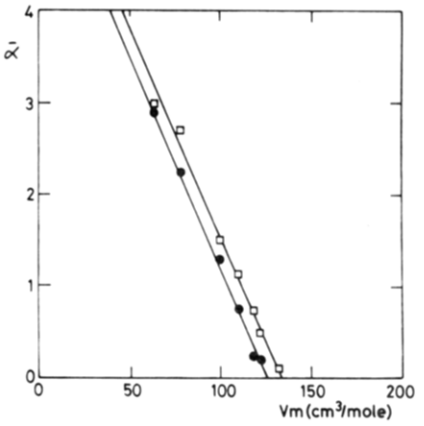

Figure 7. $\bar{\alpha}$ vs solvent molar volume for (●) iPMMA and (□) sPMMA.

the variation can be regarded as linear in both cases. Yet, depending on polymer tacticity, $\bar{\alpha}$ is quite different: $\bar{\alpha}$ = 0.25 for iPMMA; $\bar{\alpha}$ = 0.76 for sPMMA.

The same behavior is observed in all solvents. Figure 7, in which the variation of $\bar{\alpha}$ with the solvent molar volume is represented, shows a simple linear relation. This particularity means that the larger the solvent molecule, the lower $\bar{\alpha}$, and vice versa. This behavior is also accountable by the notion of a cavity, which ultimately implies the cavities in iPMMA to be smaller than those in sPMMA. We must emphasize here that we do not exactly know what the cavities are. As a matter of fact, the conformation of iPMMA or sPMMA is still under discussion.[8,24-28] However, it is usually considered that the chains adopt either an all-trans conformation (sPMMA)[26] or a near tt conformation (12/1 helix in iPMMA).[29] This gives a distance of about 0.57 nm in sPMMA between side groups that are liable to form a cavity and about 0.29 nm in iPMMA. These data are accordingly in agreement with our results.

Figure 8 shows the results gained on PHMA. As with PMMA, $\bar{\alpha}$ varies linearly with V_m. Yet the slope is different from that found with the PMMAs. At the moment we have no obvious explanation at hand to account for this discrepancy. While the larger solvation observed for the bulkiest solvent molecules can be accounted for by considering a deeper cavity for this polymer due to the larger side-group length (Figure 9), the lower solvation for the smallest solvent molecules is puzzling.

Figure 10 shows the results obtained in aPS samples (some of the results are from ref 30). As can be seen, there is still a simple relation between $\bar{\alpha}$ and V_m, yet this variation is somewhat different than those found for the PMMAs and the PHMA. Worth noticing is the crossover

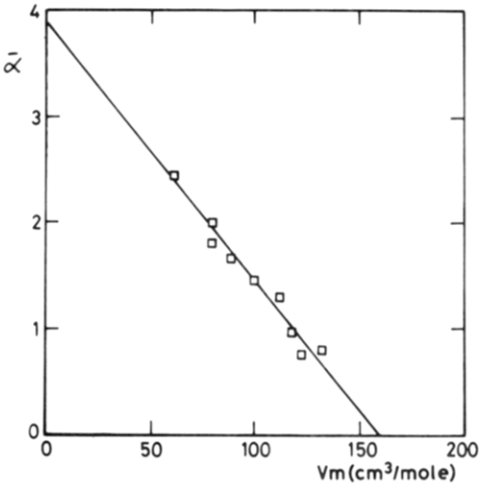

Figure 8. $\bar{\alpha}$ vs solvent molar volume for PHMA.

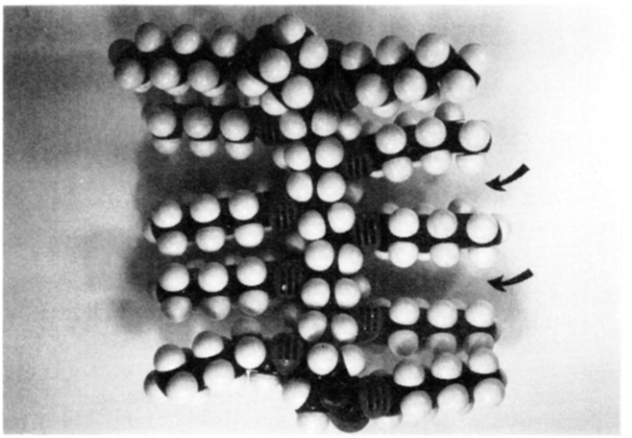

Figure 9. Representation by means of molecular models of a poly(hexyl methacrylate) under an arbitrary conformation. Arrows indicate the cavities.

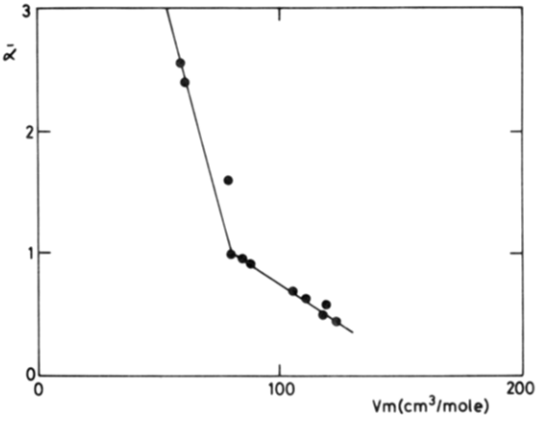

Figure 10. $\bar{\alpha}$ vs solvent molar volume for aPS.

occurring at $\bar{\alpha}$ = 1. A much higher value is found with cyclohexene, which we account for, as aforementioned, by the fact that cyclohexene does not follow the relation $V_m = \Delta H_s C^{ste}$ but is well above it.

One may wonder whether the correlation with the solvent melting temperature could not be of more significance. As a matter of fact, it can be claimed that the lower the solvent melting point, the lower the polymer concentration at which the intersection between the solvent melting line and the T_g line will occur. As a result, $\bar{\alpha}$ would become larger not on account of the smaller size of the solvent. If such were the case there should be a strong correlation between $\bar{\alpha}$ and the solvent melting point. In

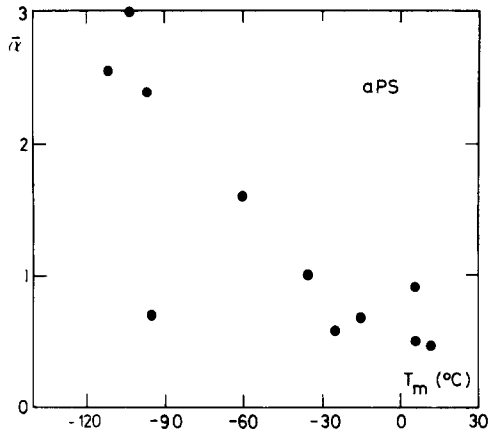

Figure 11. Representation of $\bar{\alpha}$ as a function of solvent melting temperature for aPS.

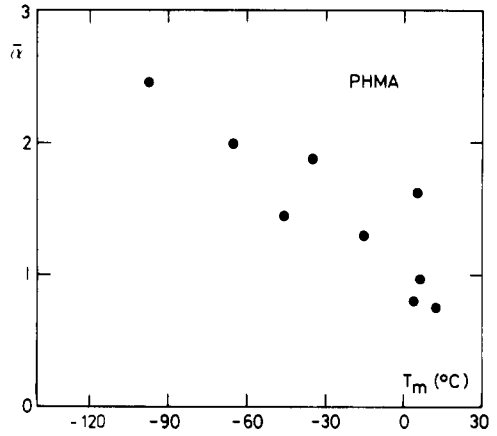

Figure 12. Representation of $\bar{\alpha}$ as a function of solvent melting temperature for PHMA.

Figures 11 and 12 are drawn the values of $\bar{\alpha}$ as a function of the solvent melting temperature. As can be seen the correlation of $\bar{\alpha}$ with V_m is in fact far better. The slight correlation seen between $\bar{\alpha}$ and T_m at low solvent melting temperatures certainly arises from the fact that V_m and T_m are then directly correlated. Conversely, it can be seen that at high solvent melting temperatures (around room temperature) the correlation between $\bar{\alpha}$ and T_m is totally absent. We accordingly estimate that it is the solvent size that matters most.

The above results provide the notion of cavity with strong support. This concept can be further tested by using polymers without bulky side groups such as PDMS and PVC which should thus not possess any cavity large enough to house solvent molecules. In addition, any effect of T_g not correlated to the solvent size can be estimated, since the glass transition temperature is some 200 °C aport. Values of $\bar{\alpha}$ reported in Table III for both polymers do show the absence of a correlation with the solvent molar volume. For instance, bromobenzene (BBz) and nitrobenzene (NBz) possess similar molar volume ($V_{m_{BBz}} \simeq 105$ cm^3, $V_{m_{NBz}} \simeq 103$ cm^3) yet $\bar{\alpha}$ varies from 0.7 to 0.4. Even if we correct by means of relation 8 the degree of crystallinity, which is about 10% whatever the solvent, the discrepancy is larger than the experimental uncertainty ($\bar{\alpha}_{BBz} = 0.83$, $\bar{\alpha}_{NBz} = 0.5$). In addition, a bulkier solvent, such as bromonaphthalene (BN) ($V_{m_{BN}} \simeq 140$ cm^3) yields $\bar{\alpha} \simeq 0.6$, a value virtually identical with that found with bromobenzene. The same behavior is observed with PDMS. Besides, with the latter polymer the values of $\bar{\alpha}$ tend to be very low, $\bar{\alpha} \simeq 0.1$ to 0.2, which is also an indication of the absence of a cavity. Worth mentioning is

Table III

solvent	V_m	$\bar{\alpha}_{PVC}$[a]	$\bar{\alpha}_{PDMS}$
bromobenzene	105	0.7	
bromonaphthalene	140	0.6	
diethyl oxalate	136	0.6	
nitrobenzene	103	0.4	
p-chlorotoluene	118		0.08
benzene	89		0.21
cyclohexane	108		1.08
trans-decalin	159		0.1

[a] From ref 40.

Table IV
Values of $\bar{\alpha}$ in iPMMA, sPMMA, PHMA, aPS, and iPS

solvent	V_m, cm^3	$\bar{\alpha}_{iPMMA}$	$\bar{\alpha}_{sPMMA}$	$\bar{\alpha}_{PHMA}$	$\bar{\alpha}_{aPS}$	$\bar{\alpha}_{iPS}$[a]
carbon disulfide	60				2.55	
methylene chloride	63	2.90	3.00	2.47	2.40	
1,2-dichloroethane	79			1.88	1.00	
chloroform	80	2.26	2.64	2.03	1.60	
benzene	89			1.64	0.92	
chlorobenzene	101	1.27	1.49	1.46		
toluene	106				0.70	
o-dichlorobenzene	112	0.75	1.13	1.31	0.64	
p-chlorotoluene	118	0.25	0.76	0.98	0.50	
cyclohexane	118				3.10	
o-xylene	120				0.59	
p-xylene	123	0.22	0.51	0.77	0.46	
2-chloro-*p*-xylene	132		0.10	0.81		
cis-decalin	154					1.75
trans-decalin	159					1.15
chlorodecane	200					0.70
chlorododecane	237					0.50

[a] From ref 11.

the comparatively high value in cyclohexane ($\bar{\alpha} \simeq 3.1$). Here the same phenomenon as with aPS + cyclohexene probably takes place, since cyclohexane, too, does not comply to the relation $V_m = \Delta HC^{ste}$ but is well above it. Note that with PDMS, we used solvents whose melting points are higher than the polymer melting point ($T_{m_{PDMS}} \simeq -58$ °C), so as to avoid interference with polymer crystallization.

From a theoretical view point, the only concept of a deformable cavity should give

$$\bar{\alpha} \simeq V_c/V_m \tag{10}$$

where V_c is the volume defined by the cavity. Whereas this relation seems to pertain to the case of polystyrenes, the linear variation in the case of PMMAs and PHMA indicates a subtler behavior. A more sophisticated approach could take into account two facts: (1) Even if a cavity is absent $\bar{\alpha}$ will not be equal to zero. The cases of PDMS and PVC illustrate this point. There is a residual constant $\bar{\alpha}_0$, which ought to be taken into account. (2) There is a cut-off solvent molar volume V_{m_0}, beyond which the solvent cannot penetrate at all the cavity even by deforming it.

Then we may have the following relation:

$$\bar{\alpha} - \bar{\alpha}_0 \simeq V_c\left(\frac{1}{V_m} - \frac{1}{V_{m_0}}\right) \tag{11}$$

This relation may look linear within experimental uncertainties in a certain range of molar volumes.

Relations 10 and 11 consider a purely geometrical problem. A more realistic approach should probably take into account energetic effects as well as the real shape of the solvent, which is here approximated to a sphere. Also, we should probably take into account the discrepancy of the solvent with respect to the relation $V_m = \Delta H_s C^{ste}$ (Figure 5).

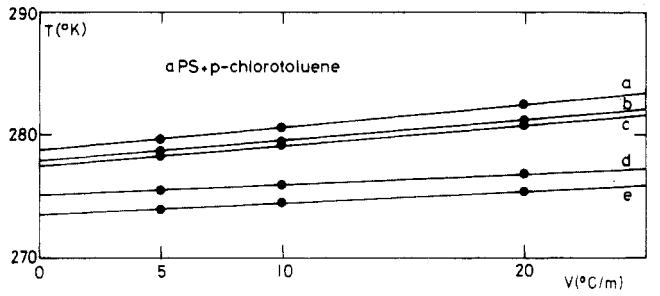

Figure 13. Representation of solvent melting temperature in aPS–*p*-chlorotoluene mixtures as a function of heating rate at different concentration of polymer: (a) 10.6%; (b) 23.45%; (c) 26.54%; (d) 42.2%; (e) 55.64%.

3. Temperature–Concentration Phase Diagrams. As has been emphasized in the Theoretical Section, the experimental value of C_g could arise from the intersection of the solvent melting line and the glass transition line. Accordingly, one may wonder whether the value of C_g is fortuitous and merely dictated by the T_g variation or whether the cavity determines both the evolution of T_g with increasing amounts of solvent and the solvent melting point with increasing polymer concentration. To examine this question more deeply, we have established the temperature–concentration phase diagrams for different polymers in the same solvent (*p*-chlorotoluene). Worth dwelling upon is the large range of glass transition temperatures which is covered: from $T_g \simeq 100$ °C (aPS and sPMMA) to $T_g \simeq -10$ °C (PHMA). The solvent melting point is taken at the maximum of the melting endotherm. The glass transition temperature is determined from the inflection point of the sample's heat capacity variation. All these results are obtained after extrapolation to zero heating rate. Typical results are given in Figure 13.

The different phase diagrams are drawn in Figure 14. As can be seen, for iPMMA, sPMMA, and aPS, C_g corresponds within experimental uncertainty to the intersection of the solvent melting line and the glass transition one. In the case of PMMA, the T_g decay is different with sPMMA than with iPMMA. As a result, the value of C_g is not the same and correspondly the value of $\bar{\alpha}$ differs. This T_g variation is linked to the expansion coefficient, which is, in turn, related to the free volume fraction.[23] Undoubtedly, this fraction is linked to the volume created by the cavity.

Interestingly enough, Kovacs and Braun[23] mention in their paper the existence of a critical concentration x_c where the T_g line, for systems rapidly quenched and heated (that is the solvent is not allowed to crystallize), should exhibit a discontinuity. The value they find experimentally for this concentration in aPS/toluene mixtures corresponds, within experimental uncertainty, to the value of C_g we found ($x_c \simeq 0.63$ g/g, $C_g \simeq 0.62$ g/g). They suggest that at x_c the polymer does not contribute any longer to the free volume of the mixture. We say that at C_g all the solvent is bound, which also implies to some extent that the polymer contribution to the free volume is zero.

The case of PHMA is still a better illustration of the cavity effect (Figure 14c). In this system, there is a discontinuity at T_g, which implies that the variation of T_g does not interfere with the solvent melting line.

The phase diagrams give additional information concerning the decrease of the solvent melting line. As developed in the Theoretical Section, this line can be calculated from relation 3 once χ is known. In practice χ can be varied between $0.3 \leq \chi \leq 0.5$, for a given polymer–solvent couple, with little influence on the T_{m_s} variation at a given concentration in the concentration range investigated. The dotted lines in Figure 14 give the theoretical variation of T_{m_s} with the solvent volume fraction. As can be seen, the fit is quite good with PDMS and iPMMA, less good with sPMMA and aPS, and in large disagreement with PHMA. Worth underlining is that with a low value of $\bar{\alpha}$ ($\bar{\alpha}_{PDMS} \simeq 0.1$ and $\bar{\alpha}_{iPMMA} \simeq 0.2$) the agreement with relation 3 is almost perfect, whereas increasing $\bar{\alpha}$ results in a larger and larger disagreement.

There are two ways of interpreting such a result. (i) The size of the solvent crystals may influence the results. It is known that below some critical size, the crystal surface free energy cannot be ignored any longer,[31] which according to Brun et al.,[32] implies a depression of the solvent melting point. To clear up this point, we have studied the crystallization of the solvent under the microscope in highly concentrated PHMA/*p*-chlorotoluene solutions. Pictures given in Figure 15 show definitely that the crystals are large enough so that this explanation can be dismissed.

(ii) The cavity effect must be taken into consideration. Two different approaches are equally worth describing.

(1) The value of χ is misevaluated. If one tries to fit the experimental results by allowing χ to take the appropriate value, one ends up with the following results: $\chi_{aPS} \simeq 0.25 \pm 0.1$; $\chi_{sPMMA} \simeq -0.1 \pm 0.1$; $\chi_{PHMA} \simeq -0.1 \pm 0.05$.

As can be seen, negative values can be found. On the basis of the cavity notion, we propose to empirically modify relation 3 as follows:

$$\frac{1}{T_{m_s}} - \frac{1}{T_{m_s}^\circ} = -\frac{R}{\Delta H_{0s}}[\log v_s + (1 - v_s) + \Lambda(1 - v_s)^2] \tag{12}$$

in which Λ has the expression

$$\Lambda = \chi\left(1 - \zeta\frac{V_c}{V_m}\right) \tag{13}$$

in which V_c is the cavity's volume, V_m the solvent molar volume, and ζ an adjustable parameter. If the problem were a purely geometrical one, ζ would be equal to unity. Relation 13 satisfies limiting conditions. If the cavity is very small, which corresponds, for instance, to PDMS, then $V_c/V_m \ll 1$ and one retrieves $\Lambda \simeq \chi$. Similarly, if the solvent's size is larger than the cavity's, which is the case, for instance, for *p*-chlorotoluene and iPMMA, then one also has $V_c/V_m \ll 1$ and as above $\Lambda \simeq \chi$.

More interestingly, relation 13 allows Λ to reach negative values if $\zeta V_c/V_m > 1$.

(2) The polymer volume fraction, v_p, may be renormalized. Here, we suggest an alternative approach, which considers a new entity, polymer + solvent (which we designate as an "amorphous polymer–solvent compound") instead of polymer on the one hand and solvent on the other hand. This implies that at C_g, the volume fraction of this entity is equal to unity. As a result, one may simply replace v_p ($v_p = 1 - v_s$) by v_p/v_g and plot T_{m_s} as a function of v_p/v_g. Here v_g is the equivalent to C_g but in volume fraction. Equation 3 can be then rewritten as

$$\frac{1}{T_{m_s}} - \frac{1}{T_{m_s}^\circ} = -\frac{R}{\Delta H_{0s}}\left[\log\left(1 - \frac{v_p}{v_g}\right) + \frac{v_p}{v_g} + \chi(v_p/v_g)^2\right] \tag{14}$$

In any case, these modified theoretical treatments give additional support to the notion of a cavity. Whereas the solution viscosity might have an influence on the amount of crystallized solvent, it has no influence on the solvent melting point, provided the crystals have grown well above a critical size. We must also underline that for solvents of lower molar volume, the discrepancy with relation 3 is

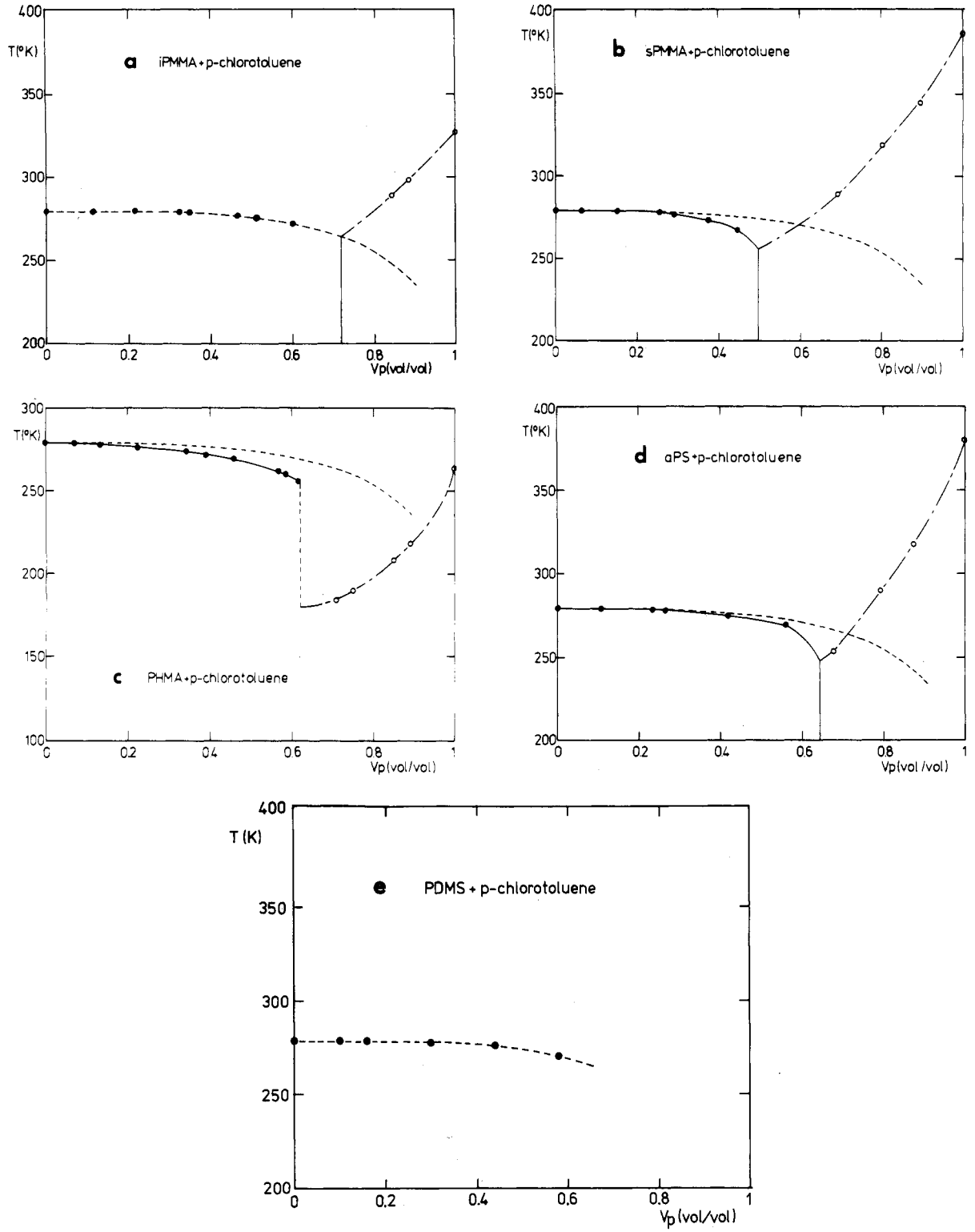

Figure 14. Temperature–concentration phase diagrams: (●) experimental solvent melting point and (○) T_g points; (- - -) theoretical variation calculated from relation 3 with $0.3 < \chi < 0.5$; (---) theoretical variation of T_g calculated from relation 5 by arbitrary taking $k = 0$, $T_{g_s} \simeq 190$ K, and $\Delta\alpha_s \simeq 5.5 \times 10^{-4}$ cm^3 g^{-1} K^{-1}. (a) iPMMA: $\Delta\alpha_p = 3.0 \times 10^{-4}$; $T_{g_p} = 326$ K. (b) sPMMA: $\Delta\alpha_p = 3.2 \times 10^{-4}$; $T_{g_p} = 386$ K. (c) PHMA: $\Delta\alpha_p = 2.5 \times 10^{-4}$; $T_{g_p} = 263$ K. (d) aPS: $\Delta\alpha_p = 3.5 \times 10^{-4}$; $T_{g_p} = 380$ K. (e) PDMS: $T_{g_p} \simeq 150$ K.

amplified (for instance $\Lambda \simeq -3 \pm 0.7$ in chloroform). These results are accordingly an independant confirmation of what has been deduced from the study of the solvent melting enthalpy.

As said above, some measurements of solvent vapor pressure in polymer solutions were carried out so as to determine χ.[19-22] As a matter of fact, the solvent chemical potential $\Delta\mu_s$ given by relation 1 can also be expressed as

$$\Delta\mu_s = RT \log (p/p_0) \qquad (15)$$

where p_0 and p are the partial pressures of the pure solvent and of the solvent in the polymer solution, respectively.

To our knowledge, the existing measurements deal with solvents of low $\bar{\alpha}$ such as aPS + *p*-chlorotoluene.[19] In the light of the results presented in this paper, it might be worth performing some experiments with a couple solvent + polymer that gives a high value of $\bar{\alpha}$ such as PHMA + *p*-chlorotoluene. In principle, the same discrepancies as those we report herein should be observed with this method.

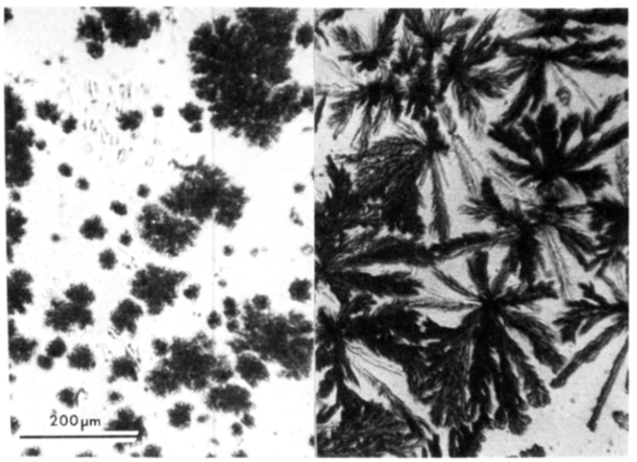

Figure 15. Optical micrographs of solvent crystalline structures in PHMA + *p*-chlorotoluene (C_p = 45%), magnification as indicated: (a) cooled at 5 °C/min down to −45 °C and kept 5 min at this temperature; (b) cooled at 20 °C/min down to −50 °C then reheated at 10 °C/min. In this case crystallization occurred on reheating, which accounts for the different morphologies.

4. Implication for Polymer Solvation. As was already emphasized in a previous publication,[30] there is not necessarily a direct correlation between $\bar{\alpha}$ and χ. For instance aPS in methylene chloride, benzene, and chlorotoluene is characterized by $\chi \simeq 0.45$–0.47, while $\bar{\alpha}$ varies from 0.5 to 2.4. We, however, note that with this polymer we have only used solvents for which $\bar{\alpha} > 0.5$. The case of PMMAs is worth examining, since values as low as 0.2 are measured. Unfortunately, the solvents giving such $\bar{\alpha}$ values have a refractive index close to that of PMMA's so that no data from light scattering (R_g, A_2) are available for calculating χ. It is, however, our feeling that these solvents, if not a Θ solvent, are either poor or marginal solvents. If such were the case this would mean that the solvent quality toward a polymer depends upon both the polymer–solvent interaction and the solvent size.

The case of iPS dilute solutions is also worth mentioning. As a matter of fact, it is known that in some solvents such as toluene the crystallization rate is exceedingly slow. To accelerate the crystallization rate, bad solvents must be used. It turns out that these bad solvents have a far larger size than toluene.[33] One of us had already explained this fact by the cavity effect:[11] toluene or decalin can enter the cavity which leads to chain "pollution" hampering "anhydrous" crystallization while larger solvents cannot, hence promoting it.

5. Cavity–Physical Gelation Relation. As said in the Introduction, it is known that the physical gelation of some polymers, particularly those with side-chain groups, occurs through the formation of polymer–solvent compounds. This view deserves further discussion on the basis of the above results.

The case of polystyrene is particularly interesting. The evolution of $\bar{\alpha}$ with V_m is similarly independent of the polystyrene tacticity, either isotactic[11] or atactic [this paper]. However, the isotactic polystyrene curve is shifted upward by a factor of 2, approximately. Note that by renormalizing either curve by the molar volume defined at $\bar{\alpha} = 1$, the curves superimpose (Figure 16). From this, we deduce that the cavity in isotactic polystyrene is larger than that in atactic polystyrene. This can be straightforwardly accounted for since, on an average, atactic polystyrene is composed of a large number of syndiotactic triads, which gives a distance between phenyl groups of

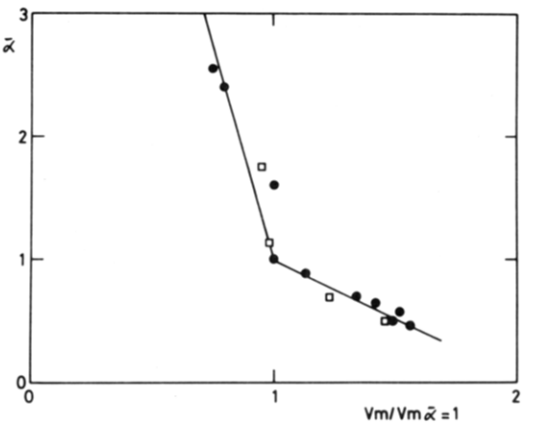

Figure 16. $\bar{\alpha}$ vs $V_m/V_{m_{\bar{\alpha}=1}}$ (renormalized curves) for (●) aPS and (□) iPS.

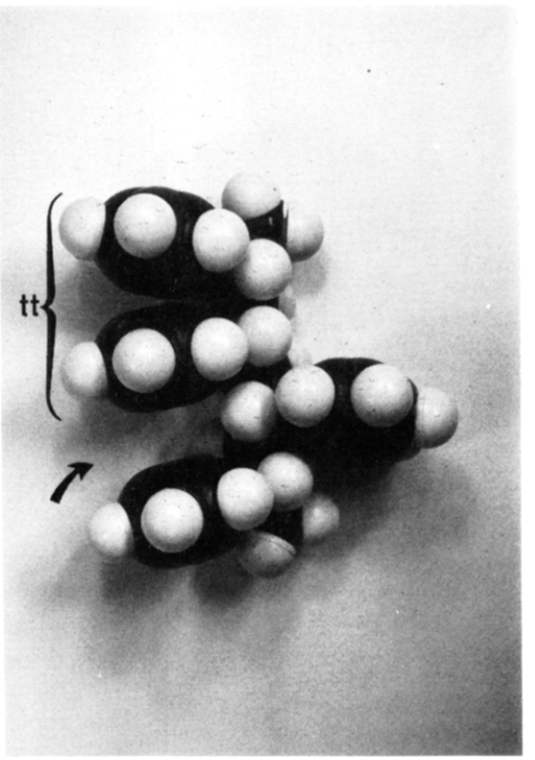

Figure 17. Representation by means of a molecular model of atactic polystyrene with an arbitrary diad arrangement. Arrow indicates the cavity formed by a syndiotactic triad; bracket indicates an isotactic arrangement adopting a tt conformation.

0.51 nm instead of 0.665 nm in iPS. In addition the presence of isotactic triads that can adopt a tt conformation[34] may lead to the absence of a cavity from place to place (Figure 17). According to the cavity's model,[11] aPS should then give physical gels in solvents of lower molar volume than those needed for iPS, which turns out to be the case. Apparently, beyond $V_m \simeq 110$ cm^3,[30] gelation does not occur any longer with aPS.

However, one ought to keep in mind that while it seems necessary to have $\bar{\alpha}$ 0.5 to produce physical gels, it is not sufficient. For instance, no gels are formed in methylene chloride although one obtains $\bar{\alpha} = 2.4$, a value very close to that found for CS_2 ($\bar{\alpha} = 2.55$). Other conditions, which we do not presently know of, are certainly required.

The case of PMMAs is more complex. Reports on the gelation of iPMMA or sPMMA concern "large" solvents such as *o*-xylene.[35,36] Since iPMMA is crystallizable, if slowly, gelation is attributed to crystallization. The low values of $\bar{\alpha}$ are consistent with this statement. Yet, one

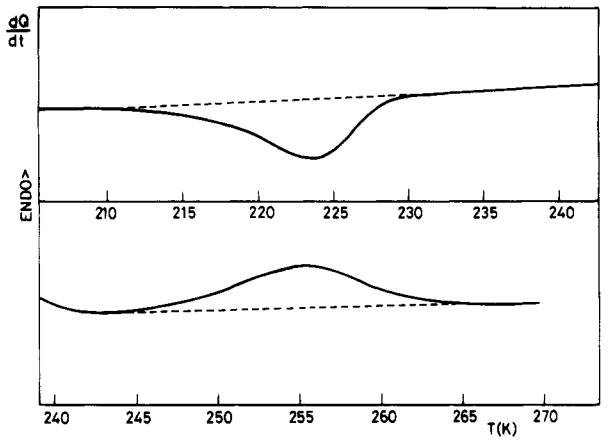

Figure 18. DSC thermogram of a 37.7% mixture iPMMA–acetonitrile. The upper curve shows the gel formation exotherm (cooling rate 5 °C/min, $\Delta H \simeq 0.98$ cal/g) and the lower curve the gel melting endotherm (heating rate 20 °C/min, $\Delta H \simeq 0.73$ cal/g).

might wonder whether polymer–solvent compounds similar to those obtained with iPS or aPS could be formed. According to the above results, this should be feasible with a small molecule. Acetonitrile seems to be a good candidate. Results drawn in Figure 18 show a gel formation exotherm and a gel melting endotherm. In addition, the melting temperature near 0 °C, a very low value for iPMMA, points to the existence of a polymer–solvent compound. Interestingly enough, acetonitrile is a Θ solvent at 30 °C.[37] In this respect the couple iPMMA–acetonitrile resembles iPS–decalin (incidentally the formation enthalpy found, $\Delta H \simeq 1$ cal/g, is also on the same order of magnitude). These results seems to indicate that provided there is no strong polymer–solvent repulsion, it is the solvent size that matters most. Finally, we must mention that while iPMMA + acetonitrile gives an unmistakable formation exotherm, nothing comparable is seen with iPMMA–*o*-xylene. Similar results have been obtained with PVC gels[38,39] and attributed to a broad spectra of crystal perfection due to the low PVC stereoregularity. Evidently, this argument cannot hold for the iPMMA sample under study. This behavior remains therefore to be accounted for.

Concluding Remarks

In this paper, we have shown that the solvent crystallization method is a reliable one, although it cannot be routinely used. The notion of a cavity due to the side groups has been investigated in polymer–solvent mixtures by means of this method. This notion has received support from both the evolution of the solvent enthalpy and the solvent melting point as a function of concentration.

It is our feeling that the conclusions we have drawn in this paper should be further investigated by means of spectroscopic techniques. Worth mentioning is that Ouano and Pecora[41,42] consider a similar cavity effect to account for their results obtained by depolarized light scattering on PMMA in chlorobenzene.

Acknowledgment. We are indebted to Dr. Wunderlich from Röhm Gmbh for kindly supplying the PMMAs samples.

Registry No. iPMMA, 25188-98-1; sPMMA, 25188-97-0; PHMA, 25087-17-6; aPS, 9003-53-6; iPS, 25086-18-4; PVC, 9002-86-2; bromobenzene, 108-86-1; bromonaphthalene, 27497-51-4; diethyl oxalate, 95-92-1; nitrobenzene, 98-95-3; *p*-chlorotoluene, 106-43-4; benzene, 71-43-2; cyclohexane, 110-82-7; *trans*-decalin, 493-02-7; carbon disulfide, 75-15-0; methylene chloride, 75-09-2; 1,2-dichloroethane, 107-06-2; chloroform, 67-66-3; chlorobenzene, 108-90-7; toluene, 108-88-3; *o*-dichlorobenzene, 95-50-1; *o*-xylene, 95-47-6; *p*-xylene, 106-42-3; 2-chloro-*p*-xylene, 95-72-7.

References and Notes

(1) Flory, P. J. *Principle of Polymer Chemistry*, Cornell University Press: Ithaca, NY, 1951.
(2) Yamakawa, H. In *Modern Theories of Polymer Solution*; Harper and Row: New York, 1971.
(3) de Gennes, P.-G. In *Scaling Concepts in Polymer Physics*; Cornell University Press: Ithaca, NY, 1979.
(4) Des Cloizeaux, J.; Jannink, G. In *Les Polymères en Solutions*; 1987 Les Editions de Physique Les Ulis; 1987.
(5) Myasnikova, R. M. *Vysokomol. Soyed.* **1977**, *19*, 564.
(6) Point, J. J.; Coutelier, C.; Villers, D. *J. Polym. Sci., Polym. Phys. Ed.* **1985**, *23*, 231.
(7) Point, J. J.; Coutelier, C.; Villers, D. *J. Phys. Chem.* **1986**, *90*, 3273.
(8) Kusuyama, H.; Miyamoto, N.; Chatani, Y.; Tadokoro, H. *Polym. Commun.* **1983**, *24*, 119.
(9) Delmas, G.; et al. *Macromolecules* **1984**, *17*, 1200; **1985**, *18*, 1235.
(10) Sundararajan, P. R.; Tyrer, N. J.; Bluhm, T. L. *Macromolecules* **1982**, *15*, 286.
(11) Guenet, J. M. *Macromolecules* **1986**, *19*, 1960.
(12) Guenet, J. M.; McKenna, G. B. *Macromolecules* **1988**, *21*, 1752.
(13) Yasuda, H.; Olf, H.; Crist, B.; Camaze, C. E.; Peterlin, A. In *Waterstructure at the Water Polymer Interface*; Jellinek, H. H. D., Ed.; Plenum Press: New York.
(14) Papkov, S. P. *Polym. Sci. USSR* **1979**, *20*, 2824.
(15) Carbonnel, L.; Guieu, R.; Rosso, J. C. *Bull. Soc. Chim.* **1970**, *8–9*, 2855.
(16) Rosso, J. C., Guieu, R.; Ponge, C.; Carbonnel, L. *Bull. Soc. Chim.* **1973**, *9–10*, 2780.
(17) Smith, P. Thesis, Groningen, 1976.
(18) Koningsveld, R.; Kleintjens, L. A. *Macromolecules* **1971**, *4*, 637.
(19) Newing, M. J. *Trans. Faraday Soc.* **1950**, *46*, 613.
(20) Bawn, C. E. H.; Freeman, R. F. J.; Kamaliddin *Trans. Faraday Soc.* **1950**, *46*, 677.
(21) Gee, G. *J. Chem. Soc.* **1947**, 280.
(22) Gee, G.; Orr, W. J. C. *Trans. Faraday Soc.* **1946**, *42*, 507.
(23) Braun, G.; Kovacs, A. J. In *Physics of non-crystalline Solids*; Proc. Intl. Conf., Delft; North-Holland Publ. Co.: Amsterdam, 1964.
(24) Kusuyama, H.; Takase, M.; Higashihata, Y.; Tseng, H. T.; Chatani, Y.; Tadokoro, H. *Polym. Commun.* **1982**, *23*, 1256.
(25) Sundararajan, P. R.; Flory, P. J. *J. Am. Chem. Soc.* **1974**, *96*, 5025.
(26) Lovell, R.; Windle, A. H. *Polymer* **1981**, *22*, 175.
(27) Yoon, D. Y.; Flory, P. J. *Macromolecules* **1976**, *9*, 299.
(28) Kirste, R. G.; Kruse, W. A.; Ibel, K. *Polymer* **1975**, *16*, 120.
(29) Kusanagi, H.; Tadokoro, H.; Chatani, Y. *Macromolecules* **1976**, *9*, 531.
(30) Gan, J. Y. S.; François, J.; Guenet, J. M. *Macromolecules* **1986**, *19*, 173.
(31) Kubelka, P. Z. *Electrochemistry* **1932**, *36*, 611.
(32) Brun, M.; Lallemand, A.; Quinson, J. F.; Eyraud, C. *Thermochim. Acta* **1977**, *21*, 59.
(33) Keith, H. D.; Vadimsky, R. G.; Padden, F. J. *J. Polym. Sci., Part A-2* **1970**, *8*, 1687.
(34) Yoon, D. Y.; Sundararajan, P. R.; Flory, P. J. *Macromolecules* **1975**, *8*, 776.
(35) Berghmans, H.; Et al. *Polymer* **1987**, *28*, 97.
(36) Könnecke, K.; Rehage, G. *Makromol. Chem.* **1983**, *184*, 2679.
(37) Cohn-Ginsberg, E.; Fox, T. G.; Maron, H. *Polymer* **1962**, *3*, 97.
(38) Yang, Y. C.; Geil, P. H. *J. Macromol. Sci.* **1983**, *B22(3)*, 463.
(39) Mutin, P. H.; Guenet, J. M. *Macromolecules* **1989**, *22*, 843.
(40) Mutin, P. H. Thesis, Strasbourg, 1986.
(41) Ouano, A. C.; Pecora, R. *Macromolecules* **1980**, *13*, 1167.
(42) Ouano, A. C.; Pecora, R. *Macromolecules* **1980**, *13*, 1173.